Observations of interstellar C2 toward Chi Oph, HD 154368, 147889 and 149404

Dishoeck, E.F. van; Zeeuw, P.T. de

Mon. Not. R. astr. Soc. (1984) **206**, 383–406

Observations of interstellar C_2 toward χ Oph, HD 154368, 147889 and 149404*

Ewine F. van Dishoeck and Tim de Zeeuw *Sterrewacht Leiden, PO Box 9513, 2300 RA Leiden, The Netherlands*

Received 1983 June 2; in original form 1983 March 29

Summary. Interstellar absorption lines of the C_2 (2–0) Phillips band at 8750 Å have been searched for in the spectra of southern stars. Seventeen lines originating from the lowest eight rotational levels have been detected toward χ Oph, and eleven lines originating from the lowest five rotational levels toward HD 154368 and 147889. No C_2 lines were seen toward HD 149404. A recently developed theory has been used to extract information about the density, temperature or strength of the radiation field in the line forming interstellar regions from the observed rotational populations. The results are compared with those obtained from other molecular observations. Toward χ Oph, the interstellar radiation field appears enhanced in the ultraviolet part of the spectrum relative to the infrared part. The C_2 data suggest a higher kinetic temperature for the material in front of HD 147889 than is inferred from radio observations.

1 Introduction

The C_2 molecule has recently become a useful tool for probing the physical conditions in diffuse interstellar clouds as a result of various observational and theoretical developments. Observationally, the construction of high-resolution spectrographs with very sensitive Reticon detectors has provided the possibility of observing molecular lines in the near-infrared with equivalent widths less than 1 mÅ. This has made it possible to detect C_2 absorption lines that originate from various rotational levels J'' of the ground state of the molecule in the spectra of several bright background stars (Hobbs 1979, 1981; Chaffee *et al.* 1980; Hobbs & Campbell 1982). On the theoretical side, the excitation mechanisms of C_2 have been analysed in detail (Chaffee *et al.* 1980; van Dishoeck & Black 1982; Black & van Dishoeck 1982). It has been shown how information about the temperature and density of the gas, and about the strength of the interstellar radiation field can be extracted from the observed rotational populations.

The mechanism for producing an enhanced excited rotational population in the homonuclear molecule is a radiative one. Molecules in the ground electronic $X^1\Sigma_g^+$ state absorb photons from the interstellar radiation field at a high rate, primarily at wavelengths 8000–

* Based on observations collected at the European Southern Observatory, La Silla, Chile.

Table 1. Information about the observed stars.

Star	Spectral class★	m_V★ (mag)	$E(B-V)$ (mag)	d (pc)	log $N(H_2)$
HD 149404	O9 Iae	5.47	0.74§	1000★★	–
HD 148184 (χ Oph)	B2 IV:pe	4.42	≈0.4¶	170¶	20.63¶
HD 154368	O9 Ia	6.13	0.76‖	1000‖	–
HD 147889	B2 V†	7.86‡	1.09‡	170††	–

★Hoffleit (1982), unless otherwise indicated, †Cohen (1973), ‡Snow *et al.* (1983), §Black (1980), ¶Frisch (1979, 1980), ‖Blades (1978), ★★Estimated from the spectral class and the visual magnitude, ††Encrenaz *et al.* (1975).

12 000 Å with excitations into the $A\,^1\Pi_u$ state. The absorptions are followed by spontaneous emission back into the vibration–rotation levels of the ground state, which may subsequently cascade down into rotational levels of the lowest vibrational state through quadrupole and intercombination transitions. These radiative processes, governed by the strength of the interstellar radiation field in the (infra)red part of the spectrum, compete with collisional (de-) excitation processes, governed by the interstellar temperature and density, in establishing the steady-state populations of the rotational levels.

Further progress has recently been made by theoretical determinations of the oscillator strength of the $C_2\,A^1\Pi_u - X^1\Sigma_g^+$ Phillips system which both enters the theoretical analysis and is needed in the conversion of the measured equivalent widths into column densities. *Ab initio* quantum chemical calculations of this quantity (van Dishoeck 1983; Pouilly *et al.* 1983; Chabalowski, Peyerimhoff & Buenker 1983) appear to have removed the confusion caused by the discrepant experimental determinations (Cooper & Nicholls 1975; Roux, Cerny & d'Incan 1976; Erman *et al.* 1982; Brault *et al.* 1982). Finally, the photodissociation processes in the C_2 molecule have been investigated theoretically as well (Pouilly *et al.* 1983), thus reducing the assumptions made in the chemistry describing the abundance of interstellar C_2.

Until now, detections of absorption lines of C_2 arising from several ($\geqslant 5$) rotational levels have been made in only a few directions, mostly in the northern hemisphere (Souza 1979; Hobbs 1979, 1981; Chaffee *et al.* 1980; Hobbs & Campbell 1982). Since an excellent echelle spectrograph has recently become available at ESO in Chile, we decided to obtain spectra in the region of the (2–0) Phillips band toward several stars in the southern sky and to search for interstellar C_2 lines. Few southern stars are known to be both bright enough ($m_V \lesssim 6$) and/or to lie behind a large enough column density or interstellar matter [$\log N(H_2) \geqslant 20.5$, $A_V \gtrsim 1$ or $E(B-V) \gtrsim 0.3$] for such C_2 observations to be successful. We selected the stars HD 148184 (χ Oph), 154368, 147889 and 149404 as four interesting and promising candidates (see Table 1).

2 Observations and reductions

The specta were obtained with the coudé echelle spectrograph fed by the 1.4-m coudé auxiliary telescope at ESO, La Silla, Chile. The detector of the spectrograph consists of a Reticon array of 1872 photodiodes cooled to 140 K and has been described elsewhere (Enard 1981). The resolving power used in the present observations was 80 000 (109.8 mÅ) corresponding to an entrance slit width of 386 μm and a dispersion of 2.45 Å mm^{-1} or 36.7 mÅ per pixel. The spectra were centred at a wavelength of 8781 Å and covered the 8745–8812 Å range, thus including all R lines of practical interest, the Q lines for $J'' \leqslant 16$

Table 2. Exposure times for the observed stars.

Star	Exposure time (hr)	No. of exposures	Date (1982)	Total exposure time (hr)
HD 149404	1	3	May 29	6
	3	1	May 29	
HD 148184 (χ Oph)	1½	3	May 30	11½
	3	1	May 30	
	4	1	June 7	
HD 154368	1½	2	June 2	11½
	3	2	June 2	
	2½	1	June 7	
HD 147889	1½	1	June 3	8½
	3	1	June 3	
	4	1	June 3	

and the P lines for $J'' \leqslant 10$ of the C_2 (2–0) Phillips band. Table 2 contains the number and duration of the exposures that were taken under conditions of average to good transmission and seeing. Each exposure was corrected by subtracting the average read-out noise of the Reticon, obtained from several noise determinations during the night. The dark current of the Reticon, which is reproducible, was subtracted as well. Several flat-field lamp spectra were taken on each night. The flat-field spectra were found to vary up to 5 per cent for some of the pixels in this wavelength region during a night. We have minimized the resulting errors by limiting the stellar exposure times, determining the flat-field spectra directly before and after each stellar exposure and checking that none of the bad pixels coincided with the C_2 lines. These flat-field spectra were then averaged and corrected for read-out noise, and the (corrected) stellar exposure was divided by the result. In order to avoid the effects of a non-uniform image remnant, the Reticon was flashed by a small lamp before any stellar, flat-field or dark integration. This small lamp uniformly saturated the Reticon; its image remnant was calibrated with time and was subtracted as well. At the beginning and end of each night a thorium spectrum was taken and used for accurate (rms = 0.001 Å) wavelength calibration by means of a least-squares polynomial fit to the lines listed by Giacchetti, Stanley & Zalubas (1970). The wavelength scale was found to vary less than half a pixel during a night, and less than a pixel over the whole observing period. The exposures on a particular star obtained on different nights were added after correction for the change in geocentric velocity of the star between the nights, and for the shift in wavelength scale.

The remaining noise in the spectra is intrinsic to the detector or may be due to weak lines of the atmospheric OH $v = 7$–3 Meinel band. The major uncertainty in the determination of the equivalent widths was therefore the location of the continuum. We estimated the continuum several times independently by eye and determined error bars corresponding to the range of continuum fits.

Column densities of C_2 in a particular rotational level J'' of the lowest vibrational level ($v'' = 0$) of the ground electronic state, $N_{J''}$, were derived from the measured equivalent widths $W_\lambda^{J'J''}$ (in Å) under the assumption of a linear relationship

$$N_{J''} = 1.13 \times 10^{20} \frac{W_\lambda^{J'J''}}{f_{J'J''}\lambda_{J'J''}^2} \text{ cm}^{-2}, \quad (1)$$

where $\lambda_{J'J''}$ is the wavelength (in Å) and $f_{J'J''}$ the absorption oscillator strength of the transition from J'' to rotational level J' of a vibrational level v' of the excited $A^1\Pi_u$ elec-

tronic state. The optically thin formula (1) is accurate to better than 10 per cent for $W_\lambda < 10$ mÅ and Doppler widths $b > 0.5$ km s^{-1} (*cf.* Strömgren 1948) for the present C_2 observations. The oscillator strength $f_{J'J''}$ can be calculated from the band oscillator strength $f_{v'v''}$ according to the formula

$$f_{J'J''} = f_{v'v''} \left\{ \frac{\nu_{J'J''}}{\nu_{\rm band}} \left[\frac{S_{J'J''}}{2(2J''+1)} \right] \right\}. \qquad (2)$$

Here $\nu_{\rm band}$ is the wavenumber of the band, equal to 11413.91 cm^{-1} for the Phillips (2–0) band, and $S_{J'J''}$ are the Hönl–London rotational line intensity factors normalized such that $\Sigma_{J'} S_{J'J''}/2(2J''+1) = 1$. For the absorption oscillator strength of the (2–0) Phillips band we used the value $f_{20} = 1.7 \times 10^{-3}$ as obtained from *ab initio* calculations (van Dishoeck 1983). Table 3 contains the rest wavelengths in air of the *P*, *Q* and *R* lines of the (2–0) Phillips band, together with the term in curly brackets in equation (2).

3 Results and interpretation

The final spectra of the four stars are presented in Fig. 1(a–d). The dominant feature in all spectra appears to be a broad stellar absorption extending from below 8745 to about 8760 Å. For HD 148184 (χ Oph), a Be star, a large emission feature with a self-absorbed core is seen at these wavelengths, which arises in the circumstellar envelope. Both the strong absorption and emission can be attributed to the H Paschen 12 ($n = 3$ to $n = 12$) line near 8750 Å. The emission plus absorption feature in the χ Oph spectrum has an equivalent width of (2.5 ± 0.1) Å. Adding to this number an estimate by eye of the equivalent width of the absorption feature of (1.5 ± 0.5) Å we find that the equivalent width of the emission feature only is (4.0 ± 0.5) Å. This is a factor of 2 below the value of 8.6 Å obtained by Briot (1981) from photographic plates with a much lower sensitivity and resolution. The spectra of HD 154368 and 149404, both O9 stars, show a second broad, less strong absorption near 8778 Å, which can be attributed plausibly to the $3p\,^3P$–$9d\,^3D$ multiplet of He I at 8776.77 Å (Moore 1949).

Superposed on the stellar features and the continuum are the small, sharp absorption lines of interstellar C_2. We did not detect other weak (interstellar) lines with more than 1–2σ certainty in this wavelength range. In particular, our spectra do not show the telluric H_2O line at 8758.42 Å, the unidentified feature around 8760 Å seen toward *o* Per (Hobbs 1981)

Table 3. Rest wavelengths (in Å) in air and the term $\{(\nu_{J'J''}/\nu_{\rm band})\,[S_{J'J''}/2(2J''+1)]\}$ for the *R*, *Q* and *P* lines of the C_2 Phillips (2–0) band system.

J''	$R(J'')$		$Q(J'')$		$P(J'')$	
	$\lambda_{\rm air}$	{ }	$\lambda_{\rm air}$	{ }	$\lambda_{\rm air}$	{ }
0	8757.686	1.000	–	–		
2	8753.949	0.400	8761.194	0.500	8766.031	0.100
4	8751.685	0.334	8763.751	0.500	8773.430	0.166
6	8750.848	0.308	8767.759	0.500	8782.308	0.192
8	8751.486	0.294	8773.221	0.499	8792.648	0.205
10	8753.578	0.286	8780.141	0.499	8804.499	0.213
12	8757.127	0.280	8788.559	0.498	8817.826	0.219
14	8762.145	0.276	8798.459	0.498	8832.679	0.222
16	8768.627	0.272	8809.841	0.497	8849.071	0.225
18	8776.607	0.270	8822.725	0.496	8866.993	0.227

★Obtained from the wavenumbers in vacuum of Chauville, Maillard & Mantz (1977).

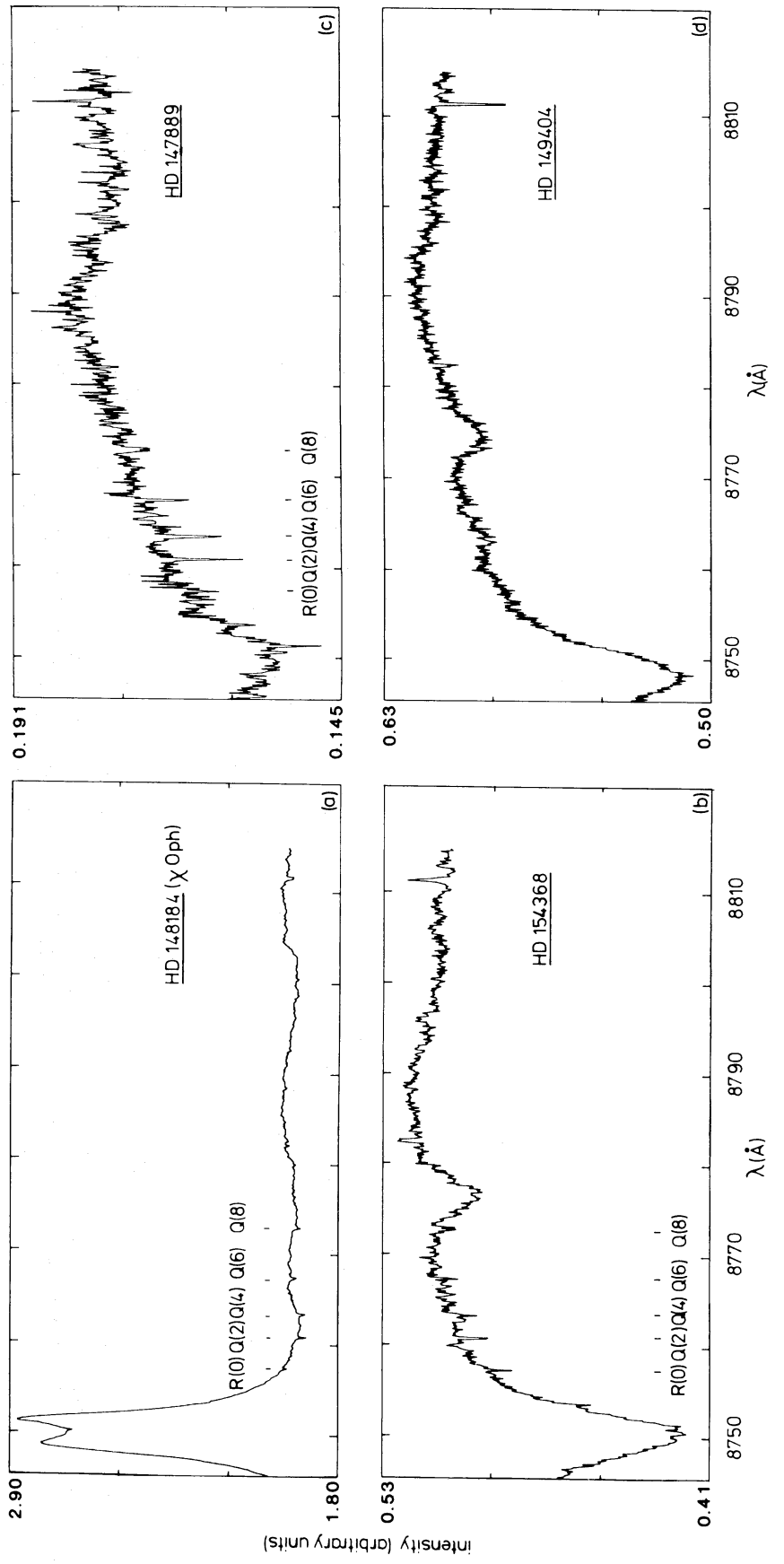

Figure 1. The spectra in the region of the (2–0) Phillips band of C_2 of (a) HD 148184 (χ Oph), (b) HD 154368, (c) HD 147889 and (d) HD 149404. The abscissa indicates wavelength with respect to a laboratory frame.

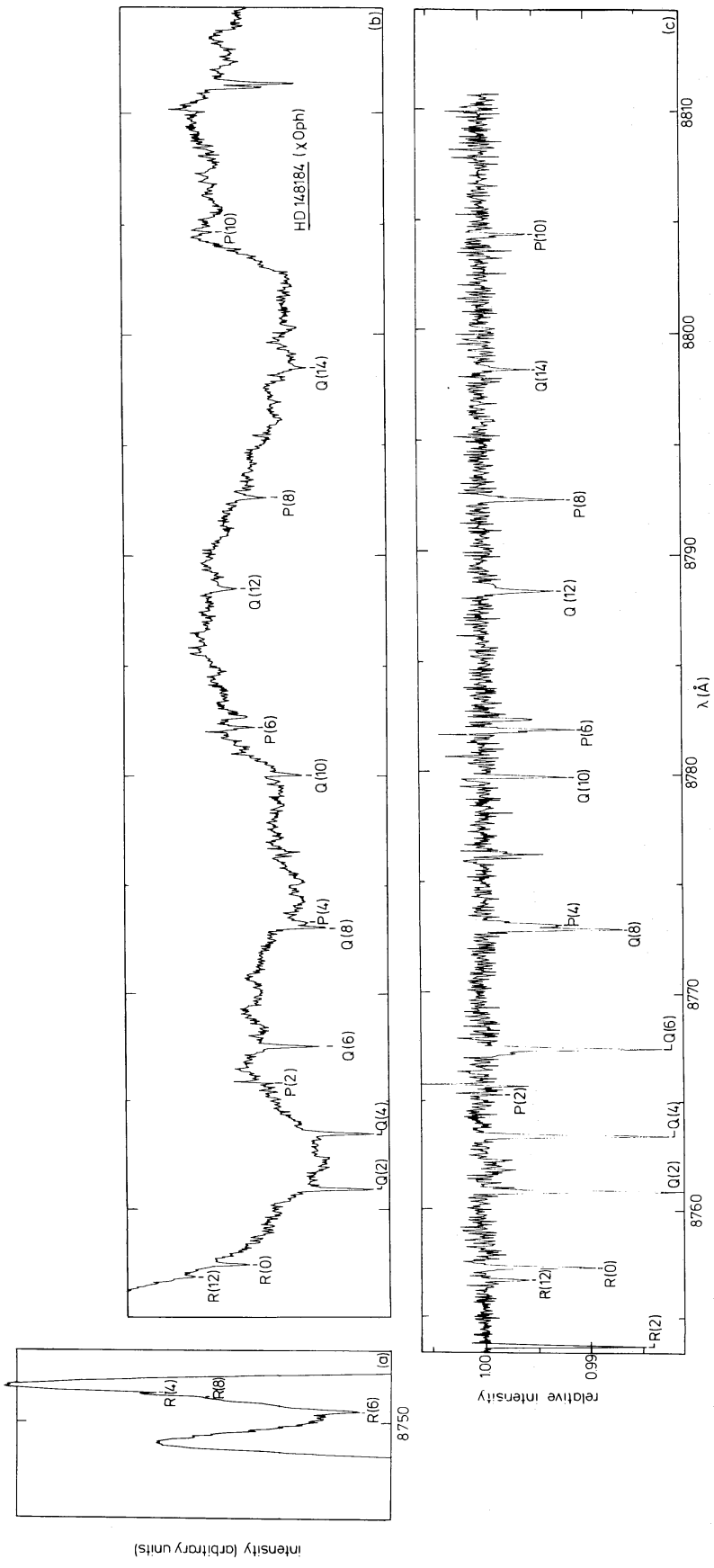

Figure 2. Enlargement of the spectrum of χ Oph as presented in Fig. 1(a). The abscissa indicates wavelength with respect to a laboratary frame. The positions of the interstellar C_2 lines of the (2–0) Phillips band are shown. (a) the 8745–8753 Å region, corresponding to the top of the H Paschen 12 emission feature; (b) the 8755–8815 Å region; (c) the rectified spectrum in the 8753–8810 Å region.

and the stellar Fe I line at 8763.98 Å. The peaks at about 8775 and 8810 Å in some of the spectra are due to bad Reticon pixels.

With the present resolution, all C_2 absorption lines appear as single lines in the spectra. Although along the line-of-sight of most of the stars atomic line observations show multiple components (Adams 1949; Frisch 1979; Blades 1978), apparently only one of the clouds contains a sufficient amount of molecules for detection. The broadening of the C_2 lines is in all cases equal to the experimental resolution, resulting in b values which are less than 3 km s^{-1}.

In the following we present and discuss the detailed results for each line-of-sight.

3.1 HD 148184 (χ Oph)

3.1.1 Results

Figs 2(a) and (b) show an enlargement of the spectrum of χ Oph as given in Fig. 1(a), with the assignment of the interstellar C_2 absorption lines. The rectified spectrum in the wavelength region between the $R(2)$ and $P(10)$ lines is shown in Fig. 2(c). The identification of the weaker lines in the spectrum was based on the accurate wavelength scale, adjusted for the Doppler shift of the strongest lines. In total, we were able to assign 17 absorption features to the P, Q or R lines of the C_2 (2–0) Phillips band, having Doppler shifts of $-(0.30 \pm 0.02)$ Å. The mean of the 17 Doppler shifts, weighted by the equivalent widths of the lines, is $-(0.300 \pm 0.005)$ Å, which, after correction for the Earth's orbital motion, yields the very accurate heliocentric radial velocity, $v_{\rm helio} = -(11.2 \pm 0.5)$ km s^{-1} for the (molecular) interstellar cloud toward χ Oph. This velocity is in good agreement with that of the molecular component identified by Frisch (1979) for which $v_{\rm helio} = -(12.1 \pm 1.0)$ km s^{-1}, and with the velocity obtained by Chaffee & White (1982), $v_{\rm helio} = -(12.2 \pm 1.0)$ km s^{-1} from atomic K I observations. Correcting as well for the Sun's motion along the line-of-sight to the star gives the radial velocity with respect to the local standard of rest (LSR), $v_{\rm LSR} = +(0.7 \pm 0.5)$ km s^{-1}. This value compares well with $v_{\rm LSR} = (1.1 \pm 0.17)$ km s^{-1} obtained by Willson (1981) from radio CH observations. It differs by about 3 km s^{-1} from the velocities determined by Jenkins, Jura & Loewenstein (1983) from observations of ultraviolet lines of C I, but this difference is comparable to the systematic errors expected in those ultraviolet measurements.

The measured equivalent widths and the derived column densities toward χ Oph are presented in Table 4. The $R(4)$, $R(6)$ and $R(8)$ lines are superposed on the Paschen 12 emission + absorption feature, while the $R(2)$ line lies on the wing of the broad emission. The $R(10)$ line should also appear on the steep part of the emission wing but is not visible. Due to the steep slope of the continuum, we were not able to obtain reliable estimates of the equivalent widths of these R lines, although results for the $R(2)$ and $R(6)$ lines are given in Table 4. The estimated (1σ) errors on the equivalent widths of the other lines are about 0.2 mÅ. The $Q(8)$ and $P(4)$ lines are separated by only 0.2 Å, i.e. twice the resolution, and are slightly blended, resulting in somewhat larger errors. The $P(2)$, $R(14)$ and $Q(16)$ lines were not detected and approximate (2σ) upper limits are given.

An independent check on the reliability of the results can be made by a comparison of the column densities derived from the P, Q and R lines which arise from the same lower level J''. As Table 4 shows, these column densities agree well, generally within the 1σ errors. The $P(2)$ line, which should have one-fifth of the strength of the $Q(2)$ line might have just been detectable. The detection of the $P(10)$ and $Q(14)$ lines is only marginal, but their derived column densities are consistent with those deduced from the $Q(10)$ line and from the upper limit on the $R(14)$ line. We emphasize that *all* C_2 lines of Table 3 which are covered in our

Table 4. Measured equivalent widths (in mÅ) and derived column densities (in 10^{12} cm^{-2}) for interstellar C_2 toward χ Oph.

J''	line	W_λ	$N_{J''}$	$\ln[N_{J''}/(2J''+1)]$	$-\ln[5N_{J''}/N_2(2J''+1)]$★
0	$R(0)$	(1.4 ± 0.1)	(1.2 ± 0.1)	(27.81 ± 0.09)	−(0.38 ± 0.10)
2	$P(2)$	≤0.5	≤4.3	≤27.48	≥−0.10
	$Q(2)$	(2.4 ± 0.1)	(4.2 ± 0.2)	(27.43 ± 0.05)	≡0
	$R(2)$	(1.7 ± 0.2)	(3.7 ± 0.5)	(27.33 ± 0.15)	(0.10 ± 0.18)
4	$P(4)$	(0.8 ± 0.2)	(4.4 ± 1.0)	(26.92 ± 0.20)	(0.52 ± 0.27)
	$Q(4)$	(2.5 ± 0.2)	(4.4 ± 0.3)	(26.92 ± 0.08)	(0.52 ± 0.12)
	$R(4)$	–	–	–	–
6	$P(6)$	(1.0 ± 0.1)	(4.5 ± 0.5)	(26.57 ± 0.10)	(0.86 ± 0.16)
	$Q(6)$	(2.4 ± 0.2)	(4.1 ± 0.4)	(26.48 ± 0.10)	(0.95 ± 0.14)
	$R(6)$	(1.3 ± 0.2)	(3.7 ± 0.4)	(26.37 ± 0.10)	(1.06 ± 0.16)
8	$P(8)$	(1.0 ± 0.1)	(4.2 ± 0.3)	(26.23 ± 0.06)	(1.20 ± 0.12)
	$Q(8)$	(2.0 ± 0.3)	(3.4 ± 0.5)	(26.02 ± 0.15)	(1.41 ± 0.19)
	$R(8)$	–	–	–	–
10	$P(10)$	(0.5 ± 0.2)	(1.7 ± 0.5)	(25.12 ± 0.35)	(2.32 ± 0.34)
	$Q(10)$	(0.8 ± 0.2)	(1.4 ± 0.3)	(24.92 ± 0.25)	(2.51 ± 0.26)
	$R(10)$	–	–	–	–
12	$Q(12)$	(0.9 ± 0.2)	(1.6 ± 0.3)	(24.88 ± 0.20)	(2.55 ± 0.27)
	$R(12)$	(0.5 ± 0.2)	(1.6 ± 0.3)	(24.88 ± 0.20)	(2.55 ± 0.25)
14	$Q(14)$	(0.6 ± 0.1)	(1.1 ± 0.2)	(24.36 ± 0.20)	(3.07 ± 0.23)
	$R(14)$	≤0.5	≤1.6	≤24.77	≥2.67
16	$R(16)$	≤0.5	≤0.9	≤24.0	≥3.35

★ The errors for $J'' \neq 2$ include the uncertainty in N_2.

spectra have either been detected or that consistent upper limits for them have been determined. Recent C_2 observations by Danks & Lambert (1983) toward χ Oph are generally in good agreement with the present measurements.

3.1.2 Interpretation

In Fig. 3, $\ln[N_{J''}/(2J''+1)]$ is plotted versus $E_{J''}/k$, where $E_{J''}$ is the energy of the rotational level J'' above level $J''=0$, and k the Boltzmann constant. It appears that the populations in the rotational levels cannot be characterized by a single rotational temperature within the error limits given in Table 4. The lowest J'' levels are described by $T_{\rm rot} \sim 65$ K, the higher levels by $T_{\rm rot} \sim 150$ K. As discussed by van Dishoeck & Black (1982), these temperatures are expected to be higher than the kinetic temperature of the gas.

The relative populations with respect to $J''=2$ are shown in the form $-\ln[5N_{J''}/N_2(2J''+1)]$ in Fig. 4 as a function of $\Delta E_{J''}/k$, where $\Delta E_{J''}$ is the excitation energy of level J'' relative to that of $J''=2$. $N_{J''=2}$ as obtained from the Q line is taken as the reference because its uncertainty is less than that of $N_{J''=0}$. The observed population ratios can be compared with theoretical predictions, *cf.* van Dishoeck & Black (1982), for a given kinetic temperature T, number density of collision partners $n = n(\mathrm{H}) + n(\mathrm{H_2})$ and scaling factor of the interstellar radiation field I.

As discussed by van Dishoeck & Black (1982), not all three parameters can be determined independently from C_2 data alone: for a given T, only the product $n\sigma_0/I$ can be obtained. The collisional cross-section σ_0 is not known from experiment or theory, but was calibrated from C_2 data toward ζ Per, together with a theoretical model of the ζ Per cloud

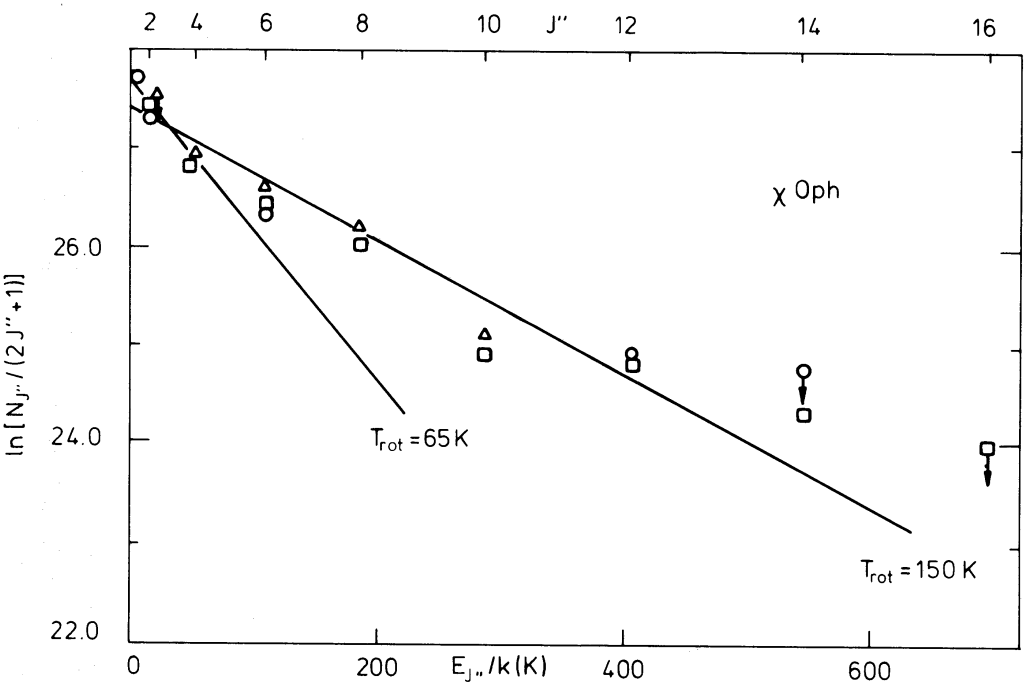

Figure 3. The C_2 rotational temperature(s) for the cloud in front of χ Oph. Δ, using N_J'' as obtained from the P line; □, using N_J'' as obtained from the Q line; ○, using N_J'' as obtained from the R line.

based on other molecular and atomic observations. This analysis resulted in $\sigma_0 \simeq 2 \times 10^{-16}$ cm^2, and we will adopt this value throughout. Its uncertainty, as estimated from the above procedure, is about 50 per cent. We also take $I = 1$, an assumption which will be discussed below. Furthermore, we have recalculated the rates of absorption out of level J'' using the new oscillator strengths for the Phillips system of van Dishoeck (1983) and those for the Mulliken system of Chabalowski *et al.* (1983). The new rates are a factor 1.35 smaller than those given by van Dishoeck & Black (1982), and can be accounted for by dividing the parameter $n\sigma_0/I$ in their tables by 1.35.

In Table 7, densities n are presented that are compatible within the stated 1σ errors, or within the 2σ errors, for a range of temperatures. It appears that the C_2 data toward χ Oph can be fitted within the 1σ errors for $T = 30$–45 K and $n = 150$–180 cm^{-3}, while the 2σ errors allow $T = 25$–70 K and $n = 150$–270 cm^{-3}. We emphasize that this range of densities does not include the uncertainty in σ_0 and is obtained with $I = 1$. If, for example, σ_0 were smaller than 2×10^{-16} cm^2, the densities would be larger by the same factor. The limits on the density are determined mainly by the high $J''(\geqslant 6)$ populations, whereas the temperature is constrained by the low J'' populations. The best theoretical fit to the C_2 data, $T \approx 40$ K and $n \approx 160$ cm^{-3} (or $n\sigma_0/I \approx 3.2 \times 10^{-14}$ cm^{-1}), is indicated in Fig. 4, together with other theoretical curves for $T = 40$ K.

There exist several studies of other atomic and molecular species toward χ Oph. Savage *et al.* (1977) measured the H_2 column densities in $J = 0$ and $J = 1$ and characterized the observed ratio by an excitation temperature of 46 K. Frisch (1979, 1980) has performed extensive visible and *Copernicus* ultraviolet observations of various atoms, ions and molecules. It appeared that the interstellar material in front of χ Oph is composed of at least five different regions having heliocentric radial velocities from -6 to -26 km s^{-1}. Various methods were used to estimate the density in the -6 to -12 km s^{-1} blend of gas, of which the molecular component is only a part, yielding conflicting results with densities $n_H = n(H) + 2n(H_2)$ varying from 60 to 10^5 cm^{-3} when a uniform temperature of 46 K was

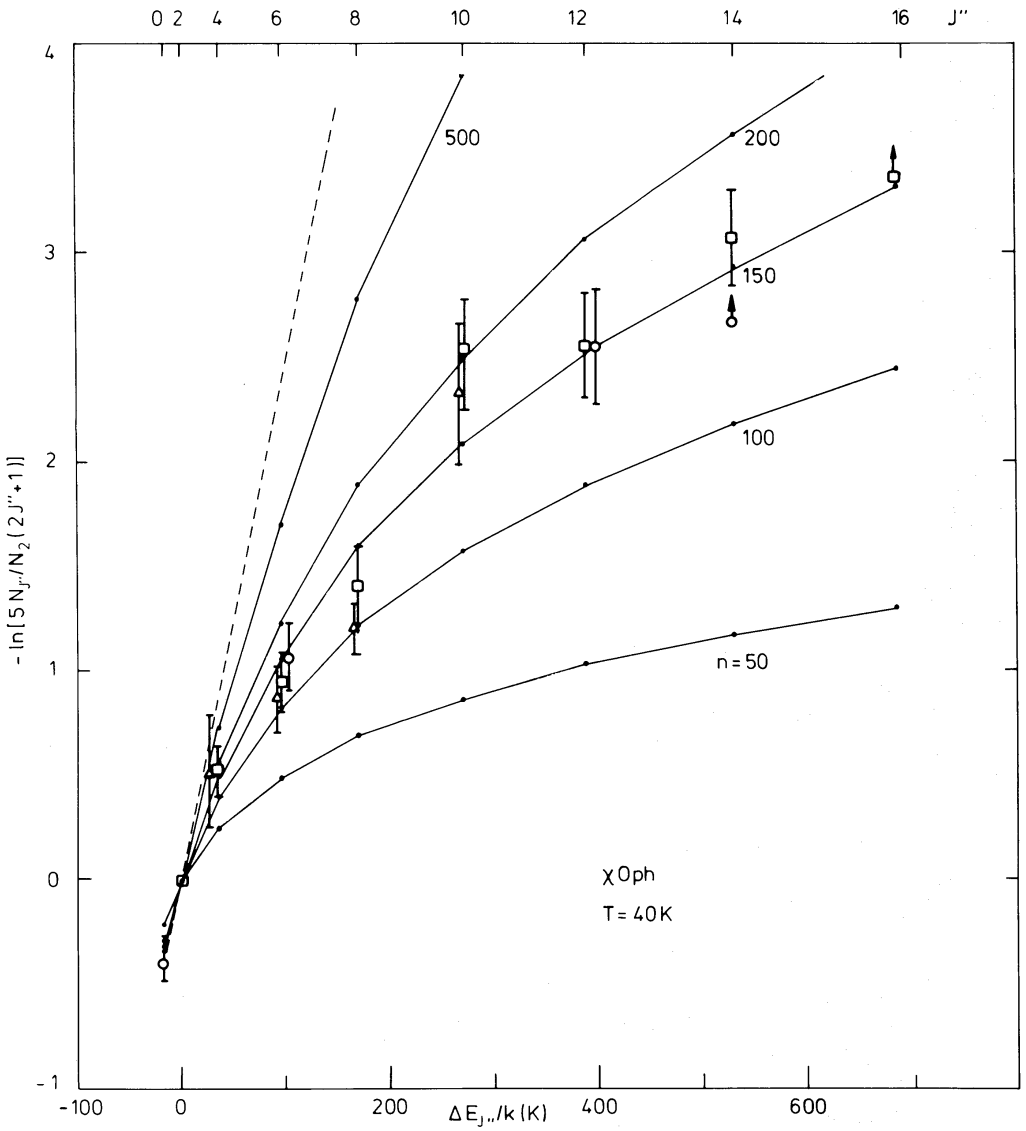

Figure 4. Observed relative rotational populations of C_2 with respect to that of the $J'' = 2$ level as functions of the excitation energy (or rotational quantum number J'') for the cloud in front of χ Oph. For explanation of the symbols, see Fig. 3. The 1σ error bars are indicated. The theoretical populations (solid lines) at a kinetic temperature $T = 40$ K are shown for comparison at several densities n, assuming $I = 1$ and $\sigma_0 = 2 \times 10^{-16}$ cm^2. The dashed line indicates the thermal distribution at 40 K. The best fit to the observational data is for $n = 160$ cm^{-3} (or $n\sigma_0/I = 3.2 \times 10^{-14}$ cm^{-1}).

assumed (see table 6 of Frisch 1980). These results were reconciled to some extent by the assumption that the gas blend represents a range of temperatures and densities, each ion or molecule probing a different region. The suggested two-component solution of a warm, low-density ($T = 300$ K, $n_H \approx 300$ cm^{-3}) and cold, high-density ($T = 46$ K, $n_H = 830$–1660 cm^{-3}) region, of which the latter would contain the neutral and molecular species, is not unique, however. The density in this model is clearly not compatible with our C_2 observations, assuming $I = 1$. Jenkins *et al.* (1983) have carried out an extensive survey of C I absorption lines using *Copernicus* in its last years of operation. Unfortunately, their data on χ Oph are of poor quality and they only give an upper limit on the pressure, $p/k < 5 \times 10^4$ cm^{-3} K, assuming a kinetic temperature of 80 K.

Since molecular hydrogen is needed for the gas-phase formation of C_2, H_2 and C_2 will belong (at least in part) to the same region of space and information about the physical conditions derived from H_2 data should apply to C_2 as well. Frisch (1980) presented column densities of H_2 in the excited rotational levels $J = 3$, 4 and 5, and an upper limit for $J = 6$. The rotational levels of H_2 are populated by a combination of ultraviolet absorption and fluorescence and subsequent infrared cascade, grain formation processes and collisional (de-) excitation. Using the formulation of Jura (1975) and assuming $T = 46$ K, Frisch derives $n_H = 85$ cm^{-3} from the observed ratio of column densities of H_2 in $J = 4$ and H. Jenkins *et al.* (1983) obtain $n > 50$ cm^{-3} with the same equation for $T = 80$ K. The assumptions that were made in this equation may not be valid, however.

A proper interpretation of the rotational populations in interstellar H_2 requires sophisticated models of the cloud structure (*cf.* Black & Dalgarno 1977; Federman, Glassgold & Kwan 1979). New, improved diffuse cloud models have been constructed in order to analyse the observational data on $H_2(J)$ and H of Frisch (1980), and details will be published separately (van Dishoeck & Black, in preparation). Preliminary results indicate that the data can be fitted within the stated errors for $T = 45$ K, $n_H \approx 250$ cm^{-3} and a scaling factor for the interstellar radiation field of about 5. The result that the column densities of all observed J levels of H_2 can be fitted with a one-component model may be due to the fact that the column density in $J = 2$ is not known, and that for $J = 3$ only within a factor of 10. However, even if the description of the populations of these levels requires a model with an additional warm, low-density region, no significant changes are expected for the parameters of the cold, dense core, where most of the C_2 resides. If we assume that $n(H) \approx n(H_2)$ in the core of the cloud, as the models suggest, then the temperature of 40 K and density $n_H = n + n(H_2) \approx 225$–$400$ cm^{-3} derived from the C_2 data agree with those from the H_2 data. However, the C_2 data assumed $I = 1$ whereas the H_2 data imply a much larger scaling factor. This apparent contradiction can be removed by noting that the C_2 excitation is mainly sensitive to the radiation field in the (infra)red part of the spectrum, whereas the H_2 data probe the ultraviolet part. The results thus indicate that the ultraviolet flux, but not the infrared flux, is enhanced in the region of the cloud. A natural explanation for this conclusion could be that the cloud is located close to the star χ Oph. The flux from the central B2 IV star at a distance d can be estimated from the model stellar atmospheres of Kurucz (1979). Taking $T_* = 20\,000$ K, $R_* = 7R_\odot$ and $\log g = 4.0$ (Panagia 1973), we find that at $d \approx 4$ pc the stellar flux in the (infra)red is well below the background interstellar flux, whereas the enhancement in the ultraviolet is still a factor 5–10. The Strömgren radius of the H II region of a B2 IV star is about $5\,n_e^{-2/3}$ pc. Although the electron density n_e (in cm^{-3}) is not known, the observed C_2 lines may well originate in the dense neutral shell compressed by and surrounding the H II region of χ Oph.

In Table 8, the abundance of C_2 relative to that of H_2, CH, CO and CN in the χ Oph cloud is given. In order to make a proper comparison between the three clouds considered in this paper, the same values for the oscillator strength have to be used in the derivation of column densities from observed equivalent widths. For CN, we scaled the data to a (0–0) band oscillator strength for the $B^2\Sigma^+$–$X^2\Sigma^+$ transition $f_{00} = 0.032$ (Cartwright & Hay 1982), and for the CH $A^2\Delta$–$X^2\Pi$ transition to $f_{00} = 0.0053$ (Brzozowski *et al.* 1976). The C_2/H_2 ratio is about 1.5 times larger than in the case of the ζ Oph cloud (compare table 2 of Hobbs & Campbell 1982), whereas the CH/C_2 ratio is about equal. The CN/C_2 ratio is at least a factor 2 smaller for the χ Oph cloud compared with other clouds. The high ultraviolet flux found for χ Oph could be a reason for the low abundance of CN, since its destruction is dominated by photodissociation in the ultraviolet region. Work on a more elaborate model of the chemistry in the χ Oph cloud is in progress (van Dishoeck & Black, in preparation).

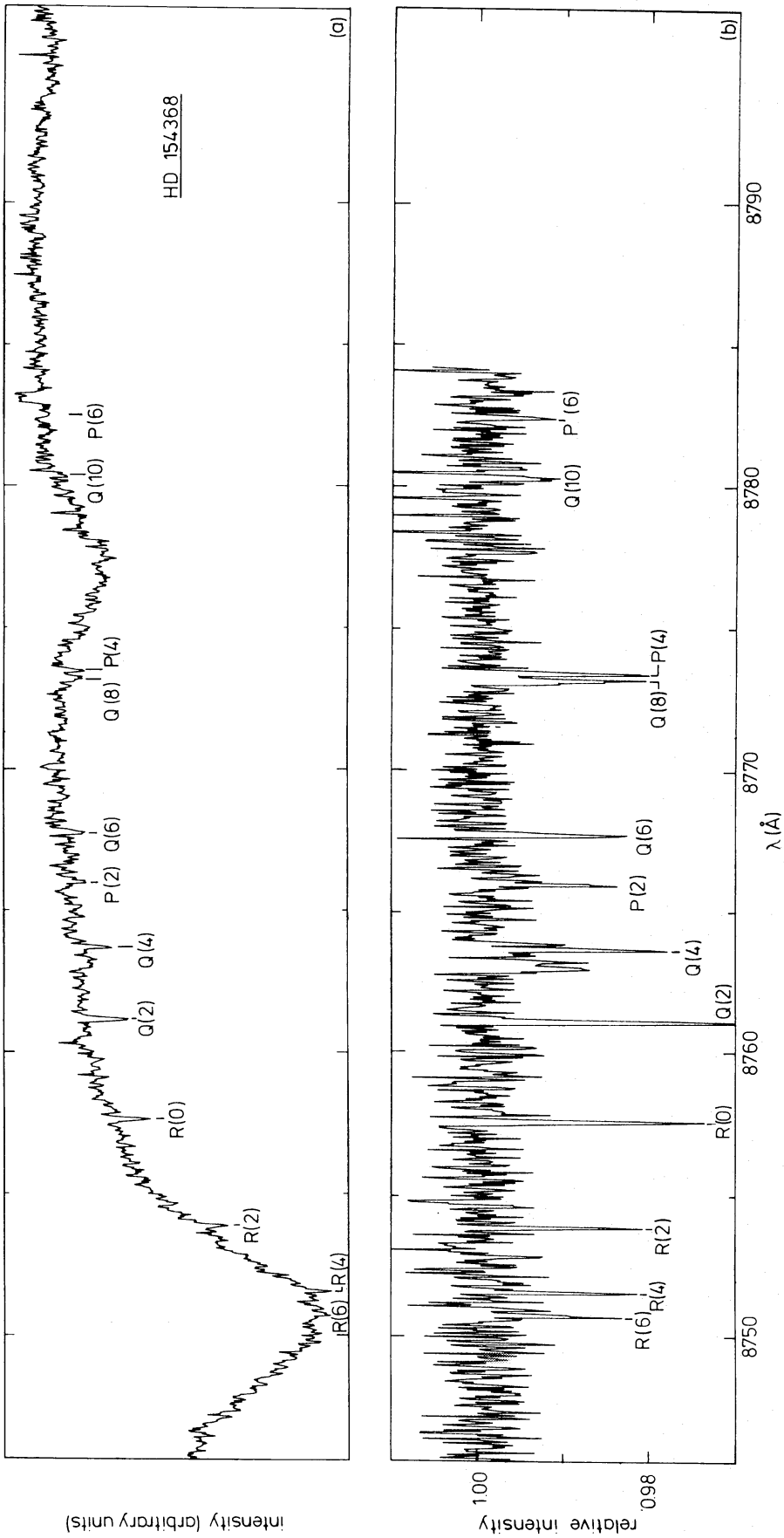

Figure 5. Enlargement of the spectrum of HD 154368 as presented in Fig. 1(b). The abscissa indicates wavelength with respect to a laboratory frame. The positions of the interstellar C_2 lines of the (2–0) Phillips band are indicated. (a) the spectrum in the 8745–8797 Å region; (b) the rectified spectrum in the 8745–8785 Å region.

Table 5. Measured equivalent widths (in mÅ) and derived column densities (in 10^{12} cm^{-2}) for interstellar C_2 toward HD 154368.

J''	Line	W_λ	$N_{J''}$	$\ln [N_{J''}/(2J''+1)]$	$-\ln [5N_{J''}/N_2(2J''+1)]$★
0	$R(0)$	(3.6 ± 0.2)	(3.1 ± 0.2)	(28.76 ± 0.07)	−(0.54 ± 0.15)
2	$P(2)$	(1.4 ± 0.2)	(12.0 ± 2.0)	(28.50 ± 0.20)	−(0.29 ± 0.26)
	$Q(2)$	(5.2 ± 0.4)	(9.0 ± 0.8)	(28.22 ± 0.10)	≡0
	$R(2)$	(3.2 ± 0.5)	(7.0 ± 1.0)	(27.97 ± 0.15)	(0.25 ± 0.23)
4	$P(4)$	(2.2 ± 0.2)	(11.7 ± 1.0)	(27.89 ± 0.10)	(0.33 ± 0.17)
	$Q(4)$	(3.8 ± 0.3)	(6.6 ± 0.6)	(27.32 ± 0.10)	(0.90 ± 0.18)
	$R(4)$	(2.2 ± 0.3)	(5.6 ± 0.6)	(27.16 ± 0.10)	(1.06 ± 0.20)
6	$P(6)$	≤1.3	≤5.8	≤26.82	≥1.30
	$Q(6)$	(3.3 ± 0.3)	(5.7 ± 0.5)	(26.81 ± 0.10)	(1.41 ± 0.18)
	$R(6)$	(1.8 ± 0.1)	(5.0 ± 0.3)	(26.68 ± 0.07)	(1.54 ± 0.15)
8	$P(8)$	≤1.3	≤5.4	≤26.48	≥1.65
	$Q(8)$	(2.3 ± 0.6)	(4.0 ± 1.0)	(26.18 ± 0.3)	(2.03 ± 0.34)
	$R(8)$	≤1.3	≤3.8	≤26.13	≥2.00
10	$P(10)$	–	–	–	–
	$Q(10)$	≤1.3	≤2.3	≤25.40	≥2.71
	$R(10)$	–	–	–	–

★See footnote to Table 4.

3.2 HD 154368

3.2.1 Results

An enlargement of the relevant part of the spectrum of HD 154368 (see Fig. 1b) is given in Fig. 5(a), while the rectified spectrum is shown in Fig. 5(b). Although in this spectrum clearly fewer C_2 lines can be identified than in the spectrum of χ Oph, still 11 lines originating from

Table 6. Measured equivalent widths (in mÅ) and derived column densities (in 10^{12} cm^{-2}) for interstellar C_2 toward HD 147889.

J''	Line	W_λ	$N_{J''}$	$\ln [N_{J''}/(2J''+1)]$	$-\ln [5N_{J''}/N_2(2J''+1)]$★
0	$R(0)$	(4.6 ± 0.2)	(4.0 ± 0.2)	(29.02 ± 0.05)	−(0.13 ± 0.11)
2	$P(2)$	(2.9 ± 0.3)	(25.5 ± 3.0)	(29.26 ± 0.12)	−(0.38 ± 0.17)
	$Q(2)$	(10.1 ± 0.6)	(17.5 ± 1.0)	(28.88 ± 0.05)	≡0
	$R(2)$	(5.3 ± 0.4)	(11.5 ± 1.0)	(29.46 ± 0.09)	(0.42 ± 0.14)
4	$P(4)$	(4.3 ± 0.3)	(22.2 ± 1.2)	(28.53 ± 0.05)	(0.35 ± 0.11)
	$Q(4)$	(13.9 ± 1.2)	(21.0 ± 1.0)	(28.62 ± 0.10)	(0.27 ± 0.14)
	$R(4)$	(8.1 ± 0.4)	(21.0 ± 1.0)	(28.48 ± 0.05)	(0.40 ± 0.10)
6	$P(6)$	(3.4 ± 0.3)	(15.3 ± 1.3)	(27.79 ± 0.08)	(1.09 ± 0.14)
	$Q(6)$	(7.8 ± 0.6)	(13.5 ± 1.0)	(27.67 ± 0.08)	(1.22 ± 0.13)
	$R(6)$	(4.0 ± 0.5)	(11.2 ± 1.5)	(27.48 ± 0.13)	(1.40 ± 0.19)
8	$P(8)$	≤2.5	≤10.5	≤27.15	≥1.68
	$Q(8)$	(4.9 ± 0.7)	(8.5 ± 1.3)	(26.94 ± 0.17)	(1.95 ± 0.21)
	$R(8)$	≤2.5	≤7.4	≤26.80	≥2.03
10	$P(10)$	–	–	–	–
	$Q(10)$	≤2.5	≤4.3	≤26.05	≥2.78
	$R(10)$	–	–	–	–

★See footnote to Table 4.

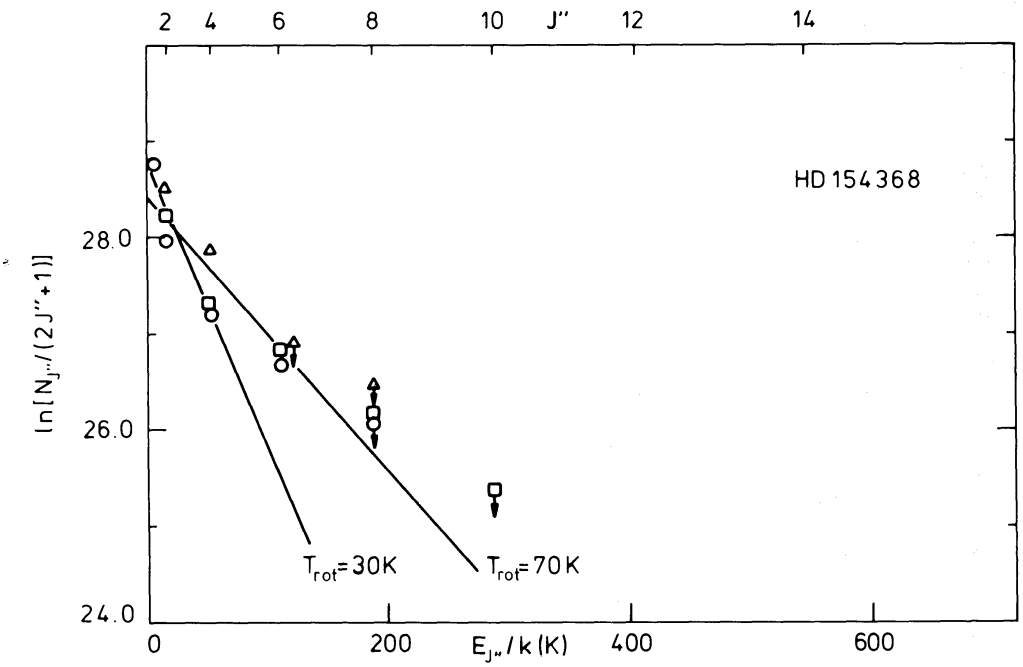

Figure 6. The C_2 rotational temperature(s) for the cloud in front of HD 154368. For explanation of the symbols, see Fig. 3.

rotational levels up to $J'' = 8$ can be seen. The R lines are again superposed on the H Paschen 12 absorption feature, but the continuum is not varying as rapidly as for χ Oph, so reliable equivalent widths should be obtainable for the R lines in this case. The weighted mean of the wavelength shifts of the 11 lines is $-(0.160 \pm 0.005)$ Å, resulting in the heliocentric velocity $v_{\rm helio} = -(2.4 \pm 0.5)$ km s^{-1}, which is in good agreement with $v_{\rm helio} = -(4.5 \pm 2.5)$ km s^{-1} obtained by Blades (1978) from observations of several atomic and molecular species. The radial velocity with respect to the LSR is $v_{\rm LSR} = +(5.5 \pm 0.5)$ km s^{-1}.

The measured equivalent widths and the derived column densities toward HD 154368 are presented in Table 5. The $P(6)$ and $R(6)$ lines are detected only at the 1σ level, whereas (2σ) upper limits for the $P(8)$, $R(8)$ and $Q(10)$ lines are given. The column densities of a particular level J'' resulting from the P, Q and R lines agree well except for the weak $P(2)$ and $P(4)$ lines, which result in too large column densities compared with those obtained from the Q and R lines. The R lines generally yield column densities that are on the low side compared with the Q lines, which may be due to a systematic error in the estimate of the continuum for the R lines.

3.2.2 Interpretation

Fig. 6 shows $\ln [N_{J''}/(2J'' + 1)]$ as a function of $E_{J''}/k$ for HD 154368. It appears that the populations of the lowest rotational levels can be characterized by a rotational temperature $T_{\rm rot} \sim 30$ K, whereas the higher levels are described by $T_{\rm rot} \sim 70$ K. We thus expect the kinetic temperature of this cloud to be low, $T < 30$ K.

Fig. 7 shows the relative populations, $-\ln [5N_{J''}/N_2(2J'' + 1)]$, as a function of $\Delta E_{J''}/k$. Following the same procedure as described for the χ Oph cloud, we can compare the observed ratios with theoretical models and derive restrictions on the temperature and density in the cloud, given values of σ_0 and I. The results, presented in Table 7, show that the C_2 data toward HD 154368 are compatible within the 1σ errors with $T = 20$–30 K and $n = 200$–255 cm^{-3}, while the 2σ errors give $T = 15$–50 K and $n = 200$–750 cm^{-3}. Note that

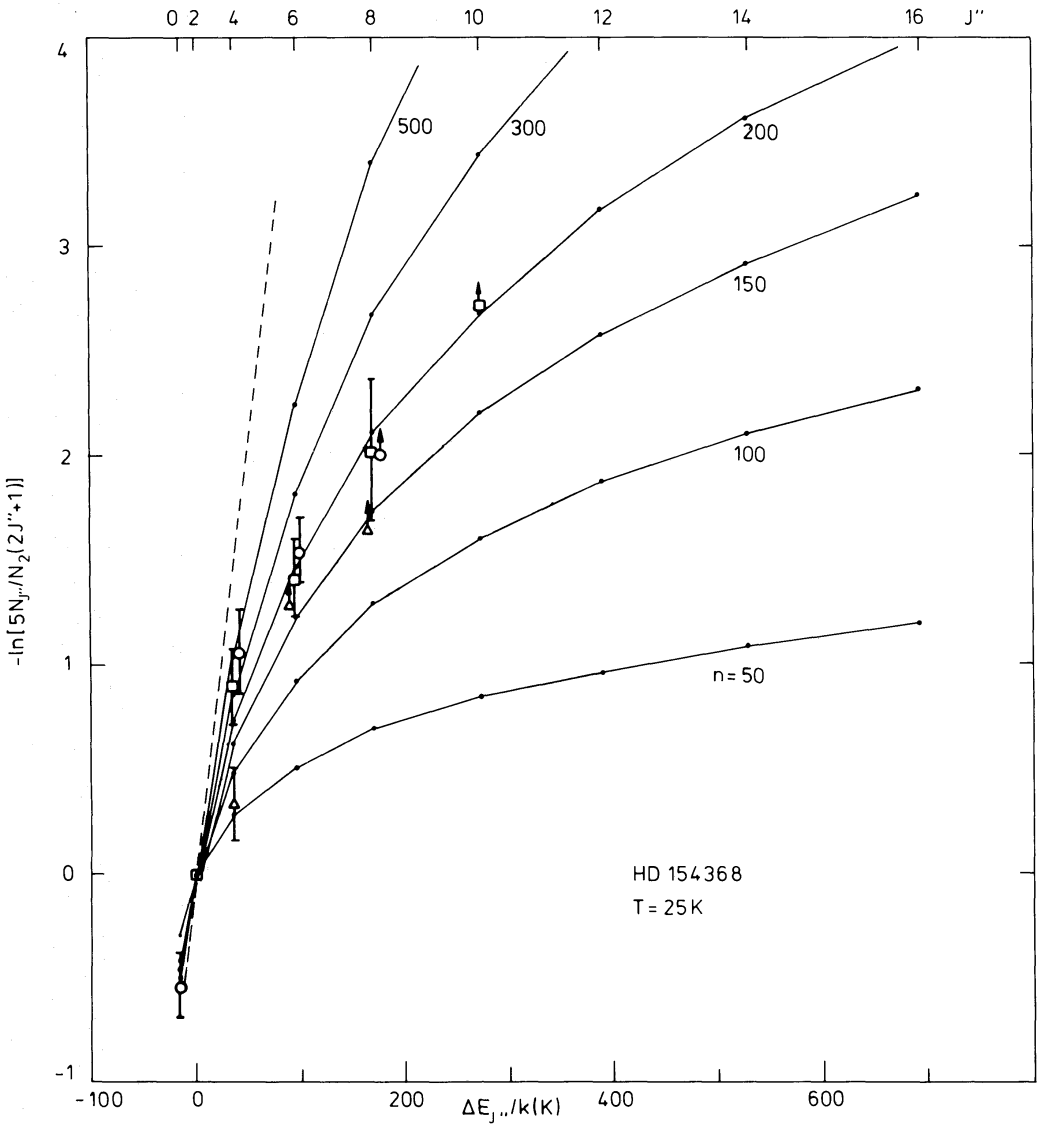

Figure 7. Observed relative rotational populations of C_2 with respect to that of the $J'' = 2$ level as functions of the excitation energy (or rotational quantum number J'') for the cloud in front of HD 154368. For explanation of the symbols, see Fig. 3. The 1σ error bars are indicated. The theoretical populations (solid lines) at a kinetic temperature $T = 25$ K are shown for comparison at several densities n, assuming $I = 1$ and $\sigma_0 = 2 \times 10^{-16}$ cm^2. The dashed line indicates the thermal distribution at 25 K. The best fit to the observational data is for $n = 225$ cm^{-3} (or $n\sigma_0/I = 4.5 \times 10^{-14}$ cm^{-1}).

the higher densities are allowed only at the higher temperatures. The best fit to the C_2 data is for $T \approx 25$ K and $n \approx 225$ cm^{-3} (or $n\sigma_0/I \approx 4.5 \times 10^{-14}$ cm^{-1}), and is illustrated in Fig. 7.

Little is known about the physical conditions in the HD 154368 cloud from other observations. Blades (1978) (see also Blades & Bennewith 1973) observed interstellar CH, CH^+ and CN lines, but measured only the excitation temperatures of these species. Although Turner & Gammon (1975) detected CN in this direction through radio observations, their radial velocity differs considerably from ours, and it is not likely that the same regions were sampled.

The relative abundances of the other molecules with respect to C_2 are given in Table 8. In contrast with the χ Oph cloud, the CN abundance toward HD 154368 is somewhat larger than in other observed regions. The CH abundance also appears unusually large. Both the CN

Table 7. Temperatures and corresponding densities★ (in cm^{-3}) compatible with C_2 observations.

Cloud	Error limits (σ)	T (K) 10	20	30	40	50	60	70	80	90	100
χ Oph	1	–	–	150	155–175	–	–	–	–	–	–
	2	–	–	150–175	155–195	160–225	170–225	175–270	–		–
HD 154368	1	–	200–245	225–255	–	–	–	–	–	–	–
	2	–	200–265	210–340	240–450	350–750	–	–	–		–
HD 147889	1	–	–	–	–	–	350–400	500–1000	>1100	–	–
	2	–	–	–	250	300–415	350–750	>500	>825	>2250	–

★ The densities $n = n(H) + n(H_2)$ are obtained using $\sigma_0 = 2 \times 10^{-16}$ cm^2 and $I = 1$. The product $n\sigma_0/I$ is actually determined by the observations (see text).

Table 8. Observed column density ratios.

Cloud	$N(C_2)$★ (10^{13} cm^{-2})	C_2/H_2 ($\times 10^{-8}$)	CH/C_2	CO/C_2	CN/C_2
χ Oph	2.5	5.9†	1.2–2.8† 1.2‡ 0.8§	14–40†	<0.05† 0.17††
HD 154368	3.4	–	7.7¶	–	1.3¶
HD 147889	7.0 7.1‖	–	1.1★★	–	–

★The total C_2 column density is obtained by summing the (mean) column densities of the observed rotational levels, and adding the contribution of the unobserved levels from the best-fitting model.
†Frisch (1979, 1980), ‡Chaffee (1975), §Willson (1981), ¶Blades (1978), ‖Souza (1979), ★★Cohen 1978, ††Danks & Lambert (1983).

and CH column densities, however, were derived with a (not well-determined) b parameter of 1.1 km s^{-1}. If the lines were unsaturated, the CN/C_2 and CH/C_2 ratios would be lowered to 0.45 and 1.6, respectively, and would agree with those found in other clouds. If the CN abundance is indeed large, this could be an indication that the flux is not enhanced in this region. These speculations could be checked by ultraviolet observations of the higher rotational levels of H_2, since they would then have a relatively low population.

3.3 HD 147889

3.3.1 Results

Fig. 8(a and b) show the enlarged (and rectified) spectrum of HD 147889. The H Paschen 12 continuum increases very gently and 11 lines originating from C_2 in rotation at levels up to $J'' = 8$ can be assigned, for which the weighted mean wavelength shift is $-(0.142 \pm 0.005)$ Å. The derived heliocentric velocity, $v_{helio} = -(7.5 \pm 0.5)$ km s^{-1}, differs considerably from $v_{helio} = -(15 \pm 3)$ km s^{-1} obtained by Cohen (1973) from atomic Na I and molecular CH observations, but agrees well with $v_{helio} = -(7.6 \pm 1.0)$ km s^{-1} obtained by Chaffee & White (1982) from atomic K I observations. The resulting LSR velocity, $v_{LSR} = +(2.7 \pm 0.5)$ km s^{-1}, also compares well with the range of velocities, $v_{LSR} = 2.5$–4.0 km s^{-1}, obtained from radio observations of molecular species in this region (Encrenaz, Falgarone & Lucas 1975).

The measured equivalent widths and the derived column densities toward HD 147889 are presented in Table 6. The agreement between the populations of a particular level J'' as obtained from the P, Q or R lines is generally acceptable, except for the $J'' = 2$ level. As was also found in the results for HD 154368, the weak $P(2)$ line gives too large, and the $R(2)$ line too small column densities compared with the strong $Q(2)$ line. The equivalent widths of the $Q(2)$ and $Q(4)$ lines are slightly larger than 10 mÅ, but the agreement between the derived column densities of the P, Q and R lines is such that the lines appear to be unsaturated. The $R(8)$ line might have just been detectable, whereas the upper limit on the $P(8)$ line is consistent with the measured equivalent width of the $Q(8)$ line.

3.2.2 Interpretation

In Fig. 9, $\ln [N_{J''}/(2J''+1)]$ is plotted against $E_{J''}/k$. The rotational populations of interstellar C_2 toward HD 147889 can be fairly well characterized by a single rotational temperature

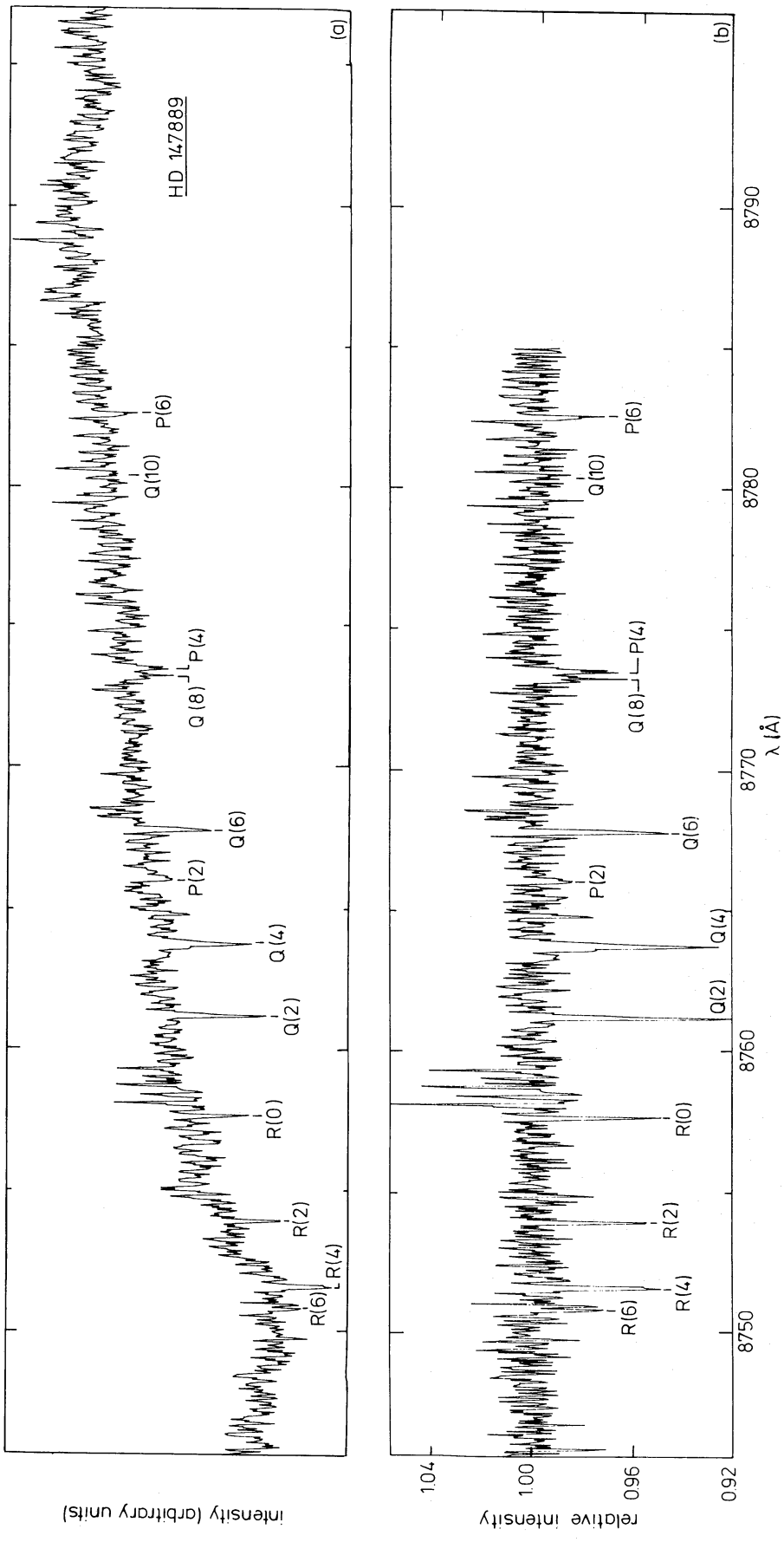

Figure 8. Enlargement of the spectrum of HD 147889 as presented in Fig. 1(c). The abscissa indicates wavelength with respect to a laboratory frame. The positions of the interstellar C_2 lines of the (2–0) Phillips band are indicated. (a) the spectrum in the 8745–8797 Å region; (b) the rectified spectrum in the 8745–8785 Å region.

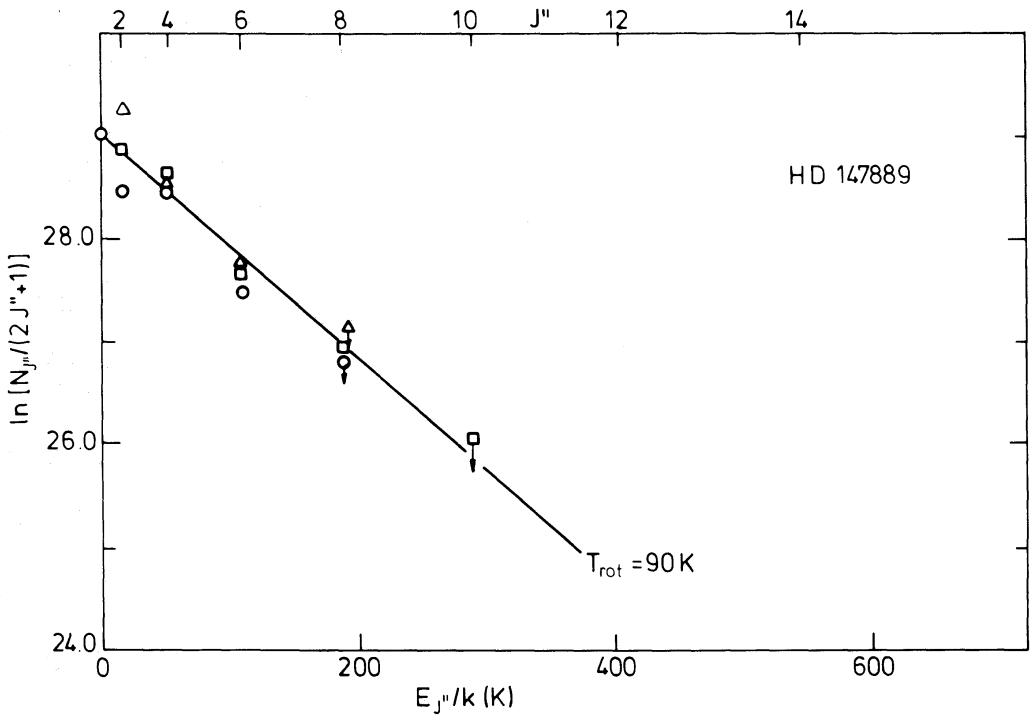

Figure 9. The C_2 rotational temperature for the cloud in front of HD 147889. For explanation of the symbols, see Fig. 3.

$T_{rot} \sim (90 \pm 20)$ K for all J''. In Fig. 10, $-\ln [5N_{J''}/N_2(2J''+1)]$ is given as a function of $\Delta E_{J''}/k$. Using again the method as described for the χ Oph cloud, we have compared the observed ratios with the theoretical predictions; the resulting constraints on the temperature and density in the HD 147889 cloud are presented in Table 7, given values for σ_0 and I. It is clear that C_2 is not a very sensitive probe for such a warm, high-density cloud as the one in front of HD 147889. The 1σ errors allow $T = 60$–90 K and $n > 350$ cm^{-3}, the 2σ errors $T = 45$–95 K and $n > 260$ cm^{-3}. Densities $n > 10^3$ cm^{-3} are only compatible with temperatures over 70 K. The best fit to the C_2 data, $T \approx 70$ K and $n \approx 700$ cm^{-3} (or $n\sigma_0/I = 1.4 \times 10^{-13}$ cm^{-1}), is illustrated in Fig. 10.

Souza (1979) has performed observations of C_2 toward HD 147889 in the (1–0) Phillips band at 10 000 Å. The derived column densities for each level $J'' = 0$, 2 and 4, and for $J'' = 6 + 8$, obtained from his equivalent widths using $f_{10} = 2.8 \times 10^{-3}$ of van Dishoeck (1983), agree with the present ones within the errors. Souza's low J'' data give a rotational temperature of about 60 K and thus provide additional support for a kinetic temperature larger than 20 K for high enough densities.

The star HD 147889 lies in the ρ Oph cloud complex, which has been studied extensively through radio observations of various molecules (Encrenaz *et al.* 1975; Myers *et al.* 1978; Gottlieb *et al.* 1978; Loren *et al.* 1979, 1980; Lada & Wilking 1980; Wootten *et al.* 1980a, b; Goldsmith & Linke 1981; Wouterloot 1981). These observations show that the ρ Oph cloud contains two separate cold, dense cores ($T \lesssim 20$ K, $n \approx 3 \times 10^5$ and $> 10^6$ cm^{-3}, respectively), located 20–30 arcmin (about 1 pc) from HD 147889, and most molecular studies have concentrated on this region. The remainder of the cloud is thought to have $T \approx 10$–25 K and $n \approx 2 \times 10^3$–10^4 cm^{-3}, although CO observations indicate the presence of a warmer region with $T = 30$–50 K located on the far side of the cloud (Loren *et al.* 1980; Lada & Wilking 1980). The density close to HD 147889 is estimated to be about 2×10^4 cm^{-3} at $T \approx 20$–30 K east of the star and less than 2×10^3 cm^{-3} for $T < 20$ K to the west (Encrenaz *et al.* 1975).

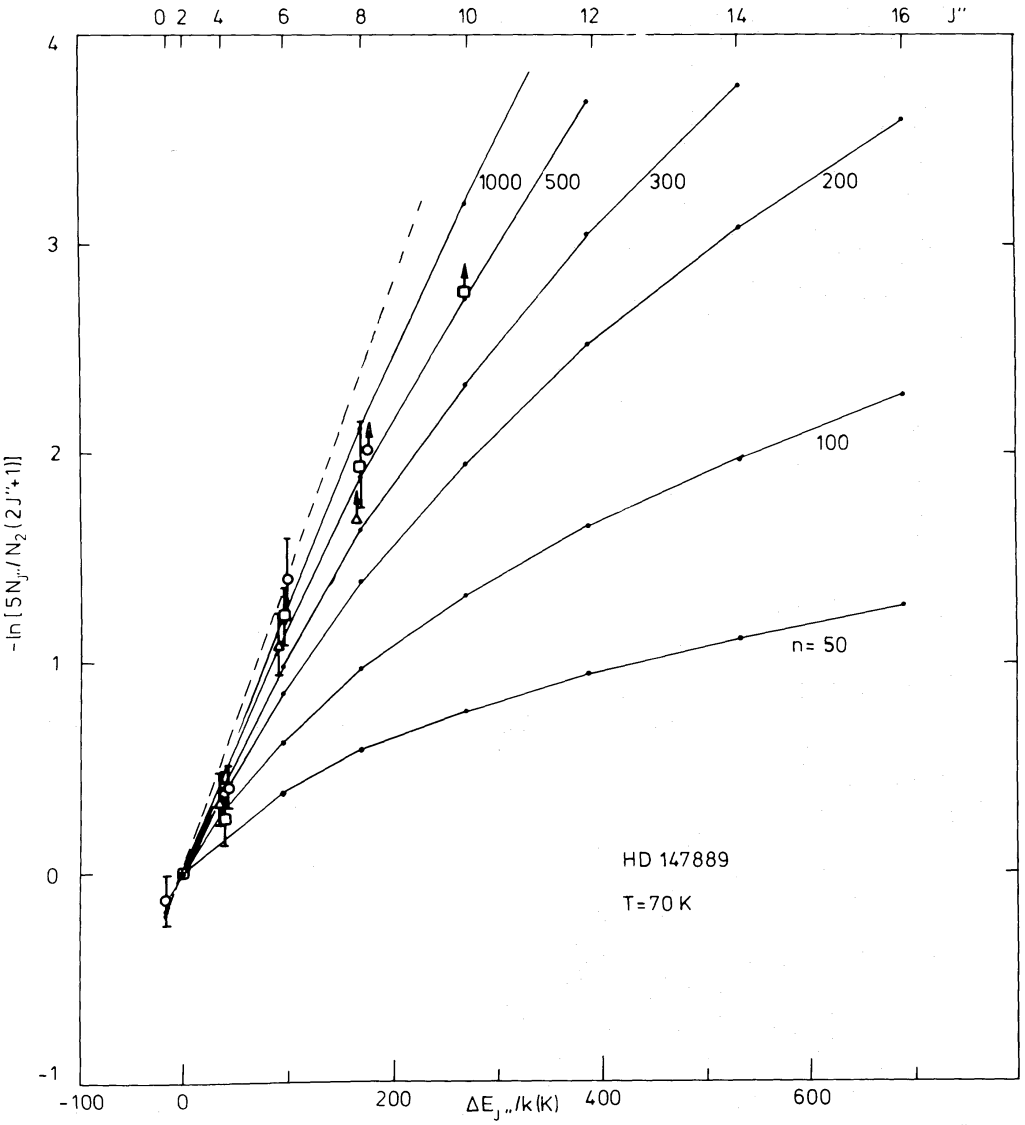

Figure 10. Observed relative rotational populations of C_2 with respect to that of the $J'' = 2$ level as functions of the excitation energy (or rotational quantum number J'') for the cloud in front of HD 147889. For explanation of the symbols, see Fig. 3. The 1σ error bars are indicated. The theoretical populations (solid lines) at 70 K are shown for comparison at several densities n, assuming $I = 1$ and $\sigma_0 = 2 \times 10^{-16}$ cm^2. The dashed line indicates the thermal distribution at 70 K. The best fit to the observational data is for $n = 700$ cm^{-3} (or $n\sigma_0/I = 1.4 \times 10^{-13}$ cm^{-1}).

The star is supposed to lie at the foremorst edge of the cloud. Myers *et al.* (1978) estimate an average density $\bar{n} \sim 10^3$ cm^{-3} around HD 147889 and Wouterloot (1981) gives $\bar{n} \approx 650$ cm^{-3}, both using $T \lesssim 20$ K. Unfortunately, no ultraviolet observations of H_2 have been performed toward this highly reddened star, to obtain information about the density and the total column density of gas in front of it. Estimates of the gas column density from the observed reddening are highly uncertain, since the extinction curve is abnormal in this direction (Bohlin & Savage 1981; Snow, Timothy & Seab 1983).

The densities obtained in the radio studies are not in contradiction with the C_2 results. The observed kinetic temperatures $T \lesssim 30$ K, however, are much lower than the value of about 70 K suggested by the C_2 data. Grasdalen, Strom & Strom (1973) (see also Vrba *et al.* 1975; Elias 1978) have discovered several point sources of infrared emission at 2 μm in the ρ Oph cloud, one of which coincides with HD 147889. Radio continuum observations at several wavelengths (Matsakis *et al.* 1976; Brown & Zuckerman 1975; Falgarone & Gilmore

1981) reveal the presence of a source at the position of the star as well. Estimates of the radius of the associated H II region vary from 0.2–0.5 pc. Encrenaz *et al.* (1975) suggest that the infrared source is capable of heating the dust and gas in the immediate surroundings (~ 0.1 pc) of the star if the density is high enough ($> 2 \times 10^4$ cm^{-3}). If the cloud were indeed located that close to the star, this could explain the higher temperature found from the C_2 data. The infrared source could also enhance the radiation field around 1 μm, where the C_2 data are sensitive, so that $I > 1$, and thus n larger by the same factor, is not excluded in this case. The radio observations, performed with a larger than 1 arcmin beam, could easily have missed such a small hotspot.

It could still be possible that the C_2 is located in a cloud which is situated well in front of the ρ Oph complex and is not associated with it. We note, however, that the radial velocities obtained from optical and radio data are in good agreement, indicating that the same regions are plausibly sampled.

The total column density of C_2 toward HD 147889 is given in Table 8. The CH/C_2 ratio appears normal in this cloud.

3.4 HD 149404

In Fig. 11 an enlargement of the spectrum of HD 149404 is given. There are no apparent strong interstellar absorption lines present in this spectrum. The spectrum shows the periodic wiggle with an amplitude of less than 1 per cent which is intrinsic to the detector. The rest wavelength positions of the C_2 lines are indicated, together with the range of positions corresponding to $-15 \leqslant v_{\text{helio}} \leqslant 15$ km s^{-1}. Buscombe & Kennedy (1962) find $v_{\text{helio}} = -7$ km s^{-1} for interstellar Ca II absorption lines in HD 149404, but this velocity may differ from that of the molecular component. It is clear that none of the C_2 lines is present in this spectrum with more than 1σ certainty. This implies that all lines have equivalent widths smaller than 1.5 mÅ. The column density of C_2 in $J'' = 0$ is thus less than 10^{12} cm^{-2}, and for $J'' > 0$ less than 2×10^{12} cm^{-2} for the line-of-sight toward HD 149404.

The star HD 149404 was selected on the basis of the great strength of ultraviolet absorption lines of interstellar CO, which suggest a column density $N(\text{CO}) \cong 6.1 \times 10^{14}$ cm^{-2} (Black 1980). The CO/C_2 ratio has been found to range from 20 to 100 in various interstellar clouds. The above mentioned value for N(CO) would imply a total column density of C_2 toward HD 149404 of 6×10^{12}–3×10^{13} cm^{-2}. This range, together with the observed upper limits for each J'', then suggests a warm, low-density region. Observations of interstellar CH might be of interest because its chemistry is related to that of C_2 (Black & Dalgarno 1977), and because of the presence of an interstellar line at 1370 Å which can tentatively be attributed to CH (Black 1980).

4 Concluding remarks

The detection of C_2 absorption lines originating from J'' up to 14 in the spectra of bright stars ($m_V \lesssim 4$) and from J'' up to 8–10 for more obscured stars ($m_V \sim 5$–8) demonstrates the excellent performance of the spectrograph and detector. Combination of the resulting high-quality data with a careful theoretical analysis of the excitation mechanism shows that the C_2 molecule is indeed a useful diagnostic tool for probing the physical conditions in interstellar clouds. The C_2 analysis is most sensitive for low temperature ($T < 50$ K) – low density ($n \lesssim 10^3$ cm^{-3}) clouds, such as χ Oph and HD 154368, and works less well, at least with the present errors on the data, for high temperature, high density clouds such as HD 147889.

The range of permitted temperatures obtained in this work can be further constrained by reducing the uncertainties for the lower J'' levels. Especially the population of the $J'' = 0$

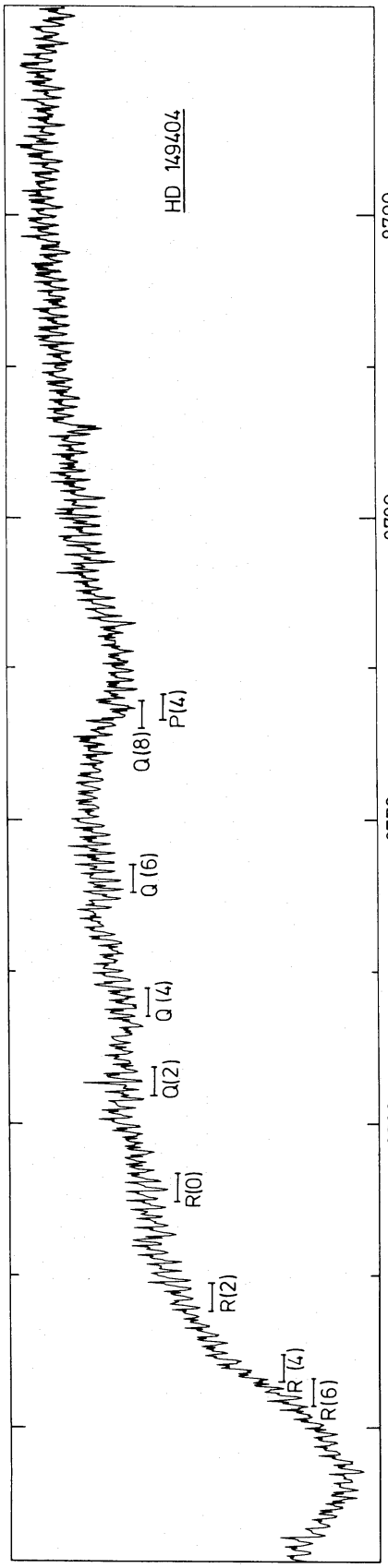

Figure 11. Enlargement of the spectrum of HD 149404 as presented in Fig. 1(d). The abscissa indicates wavelength with respect to a laboratory frame. The range of positions of each interstellar C_2 line of the (2–0) Phillips band for $-15 \leqslant v_{\rm helio} \leqslant 15$ km s^{-1} is indicated.

level, which can be derived only from one line, is critical in this respect. The parameter $n\sigma_0/I$ can be better determined by observations of lines arising from even higher J'' than in this work. For low temperature, low density regions, the populations of levels $J'' \gtrsim 10$ decrease slowly with J'' and the detection of lines from $J'' = 16$–20 should be possible in the spectra of bright stars like ζ Oph with only a small increase in sensitivity of the detector combined with a slightly larger telescope. The main uncertainty in deriving the density n, or n/I, for the cloud then remains the collisional cross-section σ_0, which has only been calibrated from astronomical observations. Moreover, the dependence of the cross-section on J'' and $\Delta J''$ has only been taken into account approximately in the theory and is a major factor of uncertainty in the analysis. Theoretical calculations and experimental determinations of these cross-sections would be of great help.

A further check on the observed rotational populations can be obtained by the observations of other bands in addition to the (2–0) band. The oscillator strength of the (3–0) Phillips band near 7720 Å, $f_{30} = 7.5 \times 10^{-4}$ (van Dishoeck 1983), is a factor 2 below f_{20}, so that detection of the stronger $R(0)$ and Q lines should be feasible. The (1–0) band near 10140 Å, and the (0–0) band near 12090 Å have much larger oscillator strengths, $f_{10} = 2.8 \times 10^{-3}$ and $f_{00} = 2.7 \times 10^{-3}$, respectively (van Dishoeck 1983). With improvements in infrared spectrometers, it might be worthwhile to try to observe these bands as well. Especially for the study of thicker interstellar clouds, the long wavelength bands are better suited because of the reduced extinction at $\lambda \geqslant 1\,\mu$m. Lines of the (1–0) band have already been detected in the highly reddened stars Cyg OB2 no. 12 and HD 147889 (Souza & Lutz 1977; Souza 1979). Another good candidate would be the star HD 29647 ($m_V = 8.3$, $E(B-V) = 1.0$) which lies in a Taurus dark cloud and for which lines of the (2–0) band have been seen (Hobbs, Black & van Dishoeck 1983; Lutz & Crutcher 1983).

The C_2 observations, and their analysis, are only one step toward the construction of models for the structure of interstellar clouds. The C_2 molecules mainly probe the dense, cold core of the cloud, and the observations are not yet accurate enough to obtain information about a (possible) warmer, less dense envelope. Additional information, especially about column densities of H, H_2 in various rotational levels and C in various fine structure levels, is needed for the constrution of more sophisticated models. Future studies of thicker clouds such as those in front of HD 147889 and 29647, which are amenable to both C_2 absorption line studies and radio observations, will be very valuable. Such studies would fill the gap between diffuse clouds investigated only optically and dark clouds studied only with radio techniques.

Acknowledgments

This work would not have been possible without the continuous interest and guidance of J. H. Black. The authors are grateful to H. J. Habing for initiating the observations and E. Maurice is thanked for assistance with the spectrograph. J. H. Black, H. J. Habing and T. de Jong commented on the manuscript. This work was supported in part by the Netherlands Organization for the Advancement of Pure Research (ZWO).

References

Adams, W. S., 1949. *Astrophys. J.*, **109**, 354.

Black, J. H., 1980. In *Interstellar Molecules, IAU Symp. 87,* p. 257, ed. Andrew, B., Reidel, Dordrecht, Holland.

Black, J. H. & Dalgarno, A., 1977. *Astrophys. J. Suppl.*, **34**, 405.

Black, J. H. & van Dishoeck, E. F., 1982. In *The Scientific Importance of Submillimetre Observations,* p. 13, ESA SP-189.

Blades, J. C., 1978. *Mon. Not. R. astr. Soc.*, **185**, 451.

Blades, J. C. & Bennewith, P. D., 1973. *Mon. Not. R. astr. Soc.*, **161**, 213.

Bohlin, R. C. & Savage, B. D., 1981. *Astrophys. J.*, **249**, 109.
Brault, J. W., Delbouille, L., Grevesse, N., Roland, G., Sauval, A. J. & Testerman, L., 1982. *Astr. Astrophys.*, **108**, 201.
Briot, D., 1981. *Astr. Astrophys.*, **103**, 5.
Brown, R. L. & Zuckerman, B., 1975. *Astrophys. J.*, **202**, L125.
Brzozowski, J., Bunker, P., Elander, N. & Erman, P., 1976. *Astrophys. J.*, **207**, 414.
Buscombe, W. & Kennedy, P. M., 1962. *Mon. Not. R. astr. Soc.*, **124**, 195.
Cartwright, D. C. & Hay, P. J., 1982. *Astrophys. J.*, **257**, 383.
Chabalowski, C. F., Peyerimhoff, S. D. & Buenker, R. J., 1983. *Chem. Phys.*, in press.
Chaffee, F. H. Jr., Lutz, B. L., Black, J. H., Van den Bout, P. A. & Snell, R. L., 1980. *Astrophys. J.*, **236**, 474.
Chaffee, F. H. Jr. & White, R. E., 1982. *Astrophys. J. Suppl.*, **50**, 169.
Chauville, J., Maillard, J. P. & Mantz, A. W., 1977. *J. Mol. Spectr.*, **68**, 399.
Cohen, J. G., 1973. *Astrophys. J.*, **186**, 149.
Cooper, D. M. & Nicholls, R. W., 1975. *J. Quant. Spectr. Rad. Transf.*, **15**, 139.
Danks, A. C. & Lambert, D. L., 1983. *Astr. Astrophys.*, **124**, 188.
Elias, J. H., 1978. *Astrophys. J.*, **224**, 453.
Enard, D. E., 1981. *The Messenger*, **26**, 22.
Encrenaz, P. J., Falgarone, E. & Lucas, R., 1975. *Astr. Astrophys.*, **44**, 73.
Erman, P., Lambert, D. L., Larsson, M. & Mannfors, B. 1982. *Astrophys. J.*, **253**, 983.
Falgarone, E. & Gilmore, W., 1981. *Astr. Astrophys.*, **95**, 32.
Federman, S. R., Glassgold, A. E. & Kwan, J., 1979. *Astrophys. J.*, **227**, 466.
Frisch, P. C., 1979. *Astrophys. J.*, **227**, 474.
Frisch, P. C., 1980. *Astrophys. J.*, **241**, 697.
Giachetti, A., Stanley, R. W. & Zalubas, R., 1970. *J. Opt. Soc. America*, **60**, 474.
Goldsmith, P. F. & Linke, R. A. 1981. *Astrophys. J.*, **245**, 482.
Gottlieb, C. A., Gottlieb, E. W., Litvak, M. M., Ball, J. A. & Penfield, H., 1978. *Astrophys. J.*, **219**, 77.
Grasdalen, G. L., Strom, K. M. & Strom, S. E., 1973. *Astrophys. J.*, **184**, L53.
Hobbs, L. M., 1979. *Astrophys. J.*, **232**, L175.
Hobbs, L. M., 1981. *Astrophys. J.*, **243**, 485.
Hobbs, L. M., Black, J. H. & van Dishoeck, E. F., 1983. *Astrophys. J.*, **271**, L95.
Hobbs, L. M. & Campbell, B., 1982. *Astrophys. J.*, **254**, 108.
Hoffleit, D., 1982. *The Bright Star Catalogue*, 4th revised edition New Haven, Yale.
Jenkins, E. B., Jura, M. & Loewenstein, M., 1983. *Astrophys. J.*, **270**, 88.
Jura, M., 1975. *Astrophys. J.*, **197**, 581.
Kurucz, R. L. 1979. *Astrophys. J. Suppl.*, **40**, 1.
Lada, C. J. & Wilking, B. A., 1980. *Astrophys. J.*, **238**, 620.
Loren, R. B., Evans, N. J. II & Knapp, G. R., 1979. *Astrophys. J.*, **234**, 932.
Loren, R. B., Wootten, A., Sandquist, Aa. & Bernes, C., 1980. *Astrophys. J.*, **240**, L165.
Lutz, B. L. & Crutcher, R. M., 1983. *Astrophys. J.*, **271**, L101.
Matsakis, D. N., Chui, M. F., Goldsmith, P. F. & Townes, C. H., 1976. *Astrophys. J.*, **206**, L63.
Moore, C. E., 1949. *Atomic Energy Levels*. vol. I, National Bureau of Standards.
Myers, P. C., Ho, P. T. P., Schneps, M. H., Chin, G., Pankonin. V. & Winnberg, A., 1978. *Astrophys. J.*, **220**, 864.
Panagia, N. 1973. *Astr. J.*, **78**, 929.
Pouilly, B., Robbe, J. M., Schamps, J. & Roueff, E., 1983. *J. Phys. B.*, **16**, 437.
Roux, F., Cerny, D. & d'Incan, J., 1976. *Astrophys. J.*, **204**, 940.
Savage, B. D., Bohlin, R. C., Drake, J. F. & Budich, W., 1977. *Astrophys. J.*, **216**, 291.
Snow, T. P., Timothy, J. G. & Seab, C. G. 1982. *Astrophys. J.*, **265**, L67.
Souza, S. P., 1979. *PhD thesis*, State University of New York, Stony Brook.
Souza, S. P. & Lutz, B., 1977. *Astrophys. J.*, **216**, L49.
Strömgren, B., 1948. *Astrophys. J.*, **108**, 242.
Turner, B. E. & Gammon, R. H., 1975. *Astrophys. J.*, **198**, 71.
van Dishoeck, E. F., 1983. *Chem. Phys.*, **77**, 277.
van Dishoeck, E. F. & Black, J. H., 1982. *Astrophys. J.*, **258**, 533.
Vrba, F. J., Strom, K. M., Strom, S. E. & Grasdalen, G. L., 1975. *Astrophys. J.*, **197**, 77.
Willson, R. C. 1981. *Astrophys. J.*, **247**, 116.
Wootten, A., Bozyan, E. P., Garrett, D. B., Loren, R. B. & Snell, R. L., 1980a. *Astrophys. J.*, **239**, 844.
Wootten, A., Snell, R. L. & Evans, N. J. II. 1980b. *Astrophys. J.*, **240**, 532.
Wouterloot, J. G. A., 1981. *PhD thesis*, Leiden University.